mathematics

Article

Solving Optimal Power Flow Problem via Improved Constrained Adaptive Differential Evolution

Wenchao Yi [1,2], Zhilei Lin [2], Youbin Lin [3], Shusheng Xiong [1,4], Zitao Yu [1,*] and Yong Chen [2]

[1] College of Energy Engineering, Zhejiang University, Hangzhou 310027, China
[2] College of Mechanical Engineering, Zhejiang University of Technology, Hangzhou 310023, China
[3] Zhejiang Chuangxin Automative Air Conditioning Company, Lishui 323799, China
[4] Longquan Industrial Innovation Research Institute, Longquan 323700, China
* Correspondence: yuzitao@zju.edu.cn

Abstract: The optimal power flow problem is one of the most widely used problems in power system optimizations, which are multi-modal, non-linear, and constrained optimization problems. Effective constrained optimization methods can be considered in tackling the optimal power flow problems. In this paper, an ϵ-constrained method-based adaptive differential evolution is proposed to solve the optimal power flow problems. The ϵ-constrained method is improved to tackle the constraints, and a p-best selection method based on the constraint violation is implemented in the adaptive differential evolution. The single and multi-objective optimal power flow problems on the IEEE 30-bus test system are used to verify the effectiveness of the proposed and improved εadaptive differential evolution algorithm. The comparison between state-of-the-art algorithms illustrate the effectiveness of the proposed and improved εadaptive differential evolution algorithm. The proposed algorithm demonstrates improvements in nine out of ten cases.

Keywords: adaptive differential evolution; optimal power flow; constrained optimization problems

MSC: 68w50

check for updates

Citation: Yi, W.; Lin, Z.; Lin, Y.; Xiong, S.; Yu, Z.; Chen, Y. Solving Optimal Power Flow Problem via Improved Constrained Adaptive Differential Evolution. *Mathematics* **2023**, *11*, 1250. https://doi.org/10.3390/math11051250

Academic Editors: Fajun Yang and Chunjiang Zhang

Received: 28 January 2023
Revised: 20 February 2023
Accepted: 28 February 2023
Published: 4 March 2023

1. Introduction

The optimal power flow (OPF) is a key problem in power system operation and control, which aims to minimize the objective function by optimizing the control variables in energy transportation and production. In the OPF, the operation cost is a fundamental basic goal, with an emphasis on sustainability and safety, the emissions and real power loss, as well as voltage stability, are also taken into account. In addition to the generator of active power, voltage magnitude, transformer tap and shunt capacitors, which can be directly controlled and need to be varied within a certain range, it is also necessary to ensure that the line loading and voltage of buses satisfy the safety constraints. Meanwhile, the presence of the equality constraints makes the OPF problem become a highly complex optimization problem. Hence, it is necessary to develop an effective algorithm to deal with OPF problems. The key objective of the OPF problem is to deal with the constraints, where the objective function should be optimized at the same time. Evolutionary algorithms have been employed to tackle the OPF variants [1–4]. Ida et al. [2] applies the multi-objective horse herd optimization to OPF. In the paper, a mechanism is proposed to update the constraint matrix in handling constraints. Bouchekara [3] improves electromagnetic field optimization (EFO) algorithm by using chaotic numbers instead of random numbers in calculation of the force of electromagnetic particles. Mugemanyi et al. [4] applied the bat algorithm in OPF. The proposed algorithm introduced the chaotic sequences to enhance its global search ability. Saha et al. [5] proposed the symbiotic organism search-based hybrid differential evolution and applied to OPF. Farhat et al. [6] proposed the neighborhood dimension learning search strategy-based slime mould algorithm and applied to OPF.

Abdel-satter et al. [7] applied the improved salp swarm algorithm (ISSA) to OPF. Taher et al. applied an improved moth flame optimization to OPF. Akdag [8] improved the Archimedes optimization algorithm and applied it to OPF. Abbasi et al. [9] combined the harmony search (HS) algorithm with the differential evolution algorithm. This method divides decision variables into ordered spans and searches. Teeparthi and Binod Kumar [10] improved the artificial physics optimization (APO) by fuzzifying the gravitational constant (G). EI-Fergany and Hasanien [11] improved the slap swarm algorithm (SSA) to tackle OPF problems. Naderi et al. [12] integrated the particle swarm optimization (PSO) with a differential evolution, and applied it to multi-objective OPF problems. Fuzzy rules help to dynamically set the inertia factor in iterations. Four fitness functions and a voltage stability based on the model analysis are considered. Elatter et al. [13] applied the Manta Ray Foraging Optimizer in OPF, where a method of selecting an ideal solution is used in the proposed algorithm. Kahraman et al. [14] introduced the crowding distance into the manta ray foraging optimization.The proposed algorithm shows a competitive performance in complex multi-objective problems. In recent years, many improved algorithms have been proposed and applied to OPF. Gong et al. [1] proposed an adaptive differential evolution to deal with the OPF, which is quite effective. Attia [15] combined the Levy flight with the sine–cosine algorithm to enhance the global searching ability, aiming at improving the efficiency of power systems. Flexible AC Transmission Systems (FACTs) are proposed, which determines the optimal location and size of FACTS devices [16]. Taking the optimal location and size of some devices into consideration, Mohamed et al. [17] combined the moth–flame optimization algorithm and gradient-based optimizer to solve OPF. This paper presents a performance evaluation of the ϵ method of the constraint handling in OPF problems. The main contribution of this paper is as follows. A constrained adaptive differential evolution is employed to address the OPF problems. A constrained mutation operator is embedded in the algorithm, which enables us to consider the constraint violation and the objective at the same time. Then, the proposed algorithm is used to tackle the OPF problems, and the experimental results illustrate the effectiveness of the algorithm.

The rest of this paper is organized as follows. Section 2 presents the proposed constrained adaptive differential evolution. Section 3 gives the mathematical model of OPF. The experimental results are presented in Section 3.1.3. Section 4 concludes the paper.

2. Adaptive Differential Evolution Based on Improved *p*best Selection

Similar to genetic algorithms, the DE consists of four operations: initialization, mutation, crossover and selection. The adaptive differential evolution (JADE) is an effective DE variant. Compared with the classical DE, both the mutation and crossover parameters in JADE are changed adaptively. A new selection strategy for the best individual is proposed to increase the population diversity. The framework of the classical JADE can be presented as follows.

2.1. Initialization

In DE, a target vector $x_{i,G}$ consisting of D dimensions is defined as an individual, where G denotes the current iteration number. $x_{i,G}$ represents a decision variable vector of the problem. During the initialization phase, NP individuals are randomly generated within the search range. Therefore, an individual represents a solution set of the constrained optimization problem. The formulation of initialization is as follows:

$$x_{i,1}^{j} = x_{min}^{j} + rand(0,1) \cdot (x_{max}^{j} - x_{min}^{j}) \tag{1}$$

where $x_{i,1}$ represents the vector of the first generation of the i-th individual. x_{min}^{j} and x_{max}^{j} denotes to the lower and upper bound of the j-th dimension,respectively. $i = 1, ..., NP$, $j = 1, ..., D$. $rand(0,1)$ represents a random number between 0 and 1.

2.2. Mutation

DE has different mutation operations to choose from. "DE/rand/1" is the most commonly used mutation strategy, which can be formulated as:

$$v_{i,G+1} = x_{r1,G} + F \cdot (x_{r2,G} - x_{r3,G}), r1 \neq r2 \neq r3 \neq i \tag{2}$$

where $v_{i,G+1}$ denotes the mutation vector. $x_{r1,G}$, $x_{r2,G}$ and $x_{r3,G}$ are three individuals randomly chosen from the G-th generation of the population. F is a mutation control parameter.

In JADE, a new mutation strategy called "DE/current-to-pbest/1" has been proven to take into account the convergence speed and global search ability, which can be formulated as:

$$v_{i,G+1} = x_{i,G} + F \cdot (x_{best,G} - x_{i,G}) + F \cdot (x_{r1,G} - x_{r2,G}), r1 \neq r2 \neq i \tag{3}$$

where $x_{best,G}$ denotes the top 100p% individuals in the current population. F is a random number that follows the Cauchy distribution with a mean of u_F and a standard deviation of 0.1. Usually u_F is initialized to 0.5.

After the mutation and crossover, the collection of all successful mutation factors F_i at each generation is denoted by S_F. Then, u_F is updated as follows:

$$u_F = (1-c) \cdot u_F + c \cdot mean_L(S_F) \tag{4}$$

where $mean_L(S_F)$ indicates that the Lehmer mean of the S_F, c is a constant between 0 and 1.

2.3. Crossover

Crossover(CR) operations create trial vectors $u_{i,G+1}$ by randomly selecting components from the target vector $x_{i,G}$ or its mutant vector$v_{i,G+1}$. The binomial crossover is typically described as

$$u^j_{i,G+1} = v^j_{i,G+1}, if \ \ rand < CR_i \ or \ j = n_j \tag{5}$$

where n_j is an integer random from 1 to D, ensuring that at least one dimension originates from the Vi mutation vector. CR_i is the crossover rate of the i-th individual, which follows the normal distribution y distribution with a mean of u_{CR} and a standard deviation of 0.1.

Similar to S_F, S_{CR} records the CR_i of successful individuals in each generation. The u_{CR} is updated as follows:

$$u_F = (1-c) \cdot u_{CR} + c \cdot mean_A(S_{CR}) \tag{6}$$

where $mean_A$ indicates the arithmetic mean of S_{CR}.

In JADE, CR_i is randomly generated and assigned to each individual. Gong et al. [18] proposed a CR sorting mechanism, which relates the CR value to individual fitness. In this process, normally distribute CR values are first randomly generated, and then the CR values and individuals fitness are arranged in ascending order, and each CR value is then assigned to an individual in order. Therefore, individuals with better fitness will assign smaller CR values, which can help the information from better individuals to survive into the next generation.

2.4. *Improved ε Method*

In the differential evolution, greedy strategies are applied to select offspring from a target vector $x_{i,G}$ and a trial vector $u_{i,G+1}$. The one with the better fitness value will survive into the next generation. The selection formula is as follows:

$$x_{i,G+1} = \begin{cases} u_{i,G+1}, & if\ f(u_{i,G+1}) \le f(x_{i,G+1}) \\ X_{i,G}, & otherwise \end{cases} \tag{7}$$

where f denotes the fitness of the individual.

The selection operator in the proposed algorithm is based on the improved ϵ-constrained methods. The ϵ-constrained methods will exaggerate the feasible region at the beginning of the evolutionary process and then narrow it down until it meets the original feasible region. In the classical ϵ-constrained method proposed by Taka [19], the ϵ-level control strategy is as follows:

$$\begin{cases} \epsilon(0) = \phi(x_\theta) \\ \epsilon(t) = \begin{cases} \epsilon(0) \cdot (1 - G/T)^{cp}, 0 < G < T \\ 0, G \ge T \end{cases} \end{cases} \tag{8}$$

where the initial value of ϵ is based on the population constraint violation level. The initial value of $\epsilon(0)$ is set as the top θth individual's constraint violation. The G-th generation ϵ value is proportion to the t and initial value of $\epsilon(0)$. When the generation G reaches a certain value T, the $\epsilon(t)$ will be set as zero. In this way, the infeasible solutions will be guided to the feasible region along the evolution process. The setting of the ϵ value is improved with the following adaptive method: However, this method ignores the information about the current population. The framework of the proposed algorithm can be presented as follows (Algorithm 1).

Algorithm 1 Improved ϵ-$JADE$

```
Initialization:NP = 50;
Generate NP individuals randomly;
Evaluate the objective function and constraint violation for each individual;
Set G = 0; FES = 0;
while FES < MaxFES do
  S_F = [];S_CR = [];
  G = G + 1;
  for each individual i in the population NP do
    CR_i = randc_i(μ_CR,0.1); F_i = randn_i(μ_F,0.1);
    Use DE/current-to-pbest/1 mutation operator to generate the mutation vector.
    Use crossover ranking technique to assign the crossover control parameter.
    Use exponential crossover to generate the trial vector.
    Apply Formula (7) to compare the trial vector with the base vector and choose the
    better one to survive into the next generation.
  end for
  Update the pbest individuals.
  Apply the Formula (8) to update the ε value
  Set FES = FES + NP
end while
```

3. Problem Formulation

This section will introduce the mathematical model of the OPF problems. The variables, constraints and objectives will be presented.

3.1. Problem Formulation

The OPF problems aim to optimize the objective function within the feasible region that satisfies the constraints. The general model of the constrained optimization problem could be formulated as follows:

$$\begin{aligned} Minimize F(x) \\ Subjectto \\ g_i(x) = 0, i = 1,2,3,...,m \\ h_j(x) \leq .0, j = 1,2,3,...,n \end{aligned} \tag{9}$$

where F is the objective function, x is the decision variable, g_i indicates the equality constraints, h_j is the inequality constraints. and m and n are the total number of equality and inequality.

3.1.1. Decision Variables

In OPF problems, the decision variables can be divided into dependent and independent variables. The independent variables can be presented as follows:

$$\begin{aligned} U = [P_G, V_G, Q_C, T_tap]_{1\times d} \\ P_G = [P_{G_1}, P_{G_2}, ..., P_{G_(N_G-1)}]_{1\times N_G} i \neq slack \\ V_G = [V_{G_1}, V_{G_2}, ..., V_{G_(N_G)}]_{1\times N_G} \\ Q_C = [Q_{C_1}, Q_{C_2}, ..., Q_{C_{N_C}}]_{1\times N_C} \\ T_tap = [T_{tap_1}, T_{tap_2}, ..., T_{tap_{N_T}}]_{1\times N_T} \\ d = (N_G - 1) + N_G + N_C + N_T \end{aligned} \tag{10}$$

where P_G denotes the output active power of the generator. N_G is the number of generators. V_G represents the voltage of the generation bus. Q_C is the injected reactive power of the shunt compensator. N_C is the number of the shunt compensators. T_tap denotes the tap setting of the transformers. NT represents the number of the transformers. d is the dimension of the decision variables. The dependent variables include the generated power of the slack bus, voltage of the load bus, load bused number, the reactive power output generators, the apparent power flow in transmission line, and the number of transmission lines. The independent variables include the output active power of the generator, generator number, voltage of the generation bus, injected reactive power of shunt compensators, the number of shunt compensator, the tap setting of transformers and the number of the transformers. The dependent variables can be given as follows:

$$X = [P_{G_0}, V_{L,1}, ..., V_{L,NPQ}, Q_{G,1}, ..., Q_{G,NPV}, S_{TL,1}, ..., S_{TL,NTL}] \tag{11}$$

3.1.2. Objective Functions

Six single objective functions of OPF and four multi-objective functions were studied in this part. The multi-objective functions are transformed into single objectives with weighted factors. The multi-objective method can be used to tackle the objectives [20].

Case 1: Fuel cost minimization

The fuel cost ($/h) is the most commonly used objective in OPF problems. The quadratic function is employed to model the generation cost.

The formulas can be given as follows:

$$F_1(X) = \sum_{i=1}^{NG} (a_i \cdot P_{G_i}^2 + b_i \cdot P_{G_i}^2 + c_i) \tag{12}$$

where the a_i, b_i and c_i are the cost coefficients of the i-th generator.

Case 2: Fuel cost with valve point-effect minimization

The fuel cost with valve point-effect and prohibited zones is used to describe the generation cost. It consists of two parts. One of them is the total fuel cost F_1, and the other is a sinusoidal function. A sinusoidal function is used to simulate the valve effect.

$$F_C = \sum_{i=1}^{NG} (a_i \cdot P_{G_i}^2 + b_i \cdot P_{G_i}^2 + c_i) + \left| d_i \cdot sin(e_i \cdot (P_{G_i}^{min} - P_{G_i})) \right| \tag{13}$$

where the d_i and e_i are the fuel cost coefficients of the i-th generator with valve-point effects. The input flow of the steam is adjusted by the generation units to control the output flow by different valves.

Case 3: Voltage stability minimization

The voltage is an important index in power system stability, which should be varied within a suitable region. Hence, the load bus L-index is used, whose value should be within the range of 0 to 1. The formula can be given as follows:

$$\begin{aligned} L_j &= \left| 1 - \sum_{i=1}^{NG} F_{ij} \cdot V_i / V_j \right|, j = 1, \ldots NL. \\ F_{V-stability} &= max(L_j), j = 1, \ldots NL. \end{aligned} \tag{14}$$

where V_i and represent the voltage of the i-th generator and j-th P-Q bus, respectively; $F_{ij}$is calculated from the X-matrix.

Case 4: Emission minimization

The emission in the power system is an important environmental index that is highly related to global warming and carbon emission issues. Hence, the emission in this case is formulated with the following formula:

$$F_E = \sum_{i=1}^{NG} \alpha_i + \beta_i \cdot P_{G_i} + \gamma_i \cdot P_{G_i}^2 + \delta_i \cdot e^{\phi_i P_{G_i}} \tag{15}$$

where $\alpha_i, \beta_i, \gamma_i, \delta_i$ and ϕ_i represent the i-th generator emission coefficients, and their values are provided in Table 1.

Table 1. Cost and emission coefficients of generators for the IEEE 30-bus system.

Generator	Bus	a	b	c	d	e	alpha	beta	gamma	w	mu
G1	1	0	2	0.00375	18	0.037	4.091	−5.554	6.49	0.0002	2.857
G2	2	0	1.75	0.0175	16	0.038	2.543	−6.047	5.638	0.0005	3.333
G3	5	0	1	0.0625	14	0.04	4.258	−5.094	4.586	0.000001	8
G4	8	0	3.25	0.00834	12	0.045	5.326	−3.55	3.38	0.002	2
G5	11	0	3	0.025	13	0.042	4.258	−5.094	4.586	0.000001	8
G6	13	0	3	0.025	13.5	0.041	6.131	−5.555	5.151	0.00001	6.667

Case 5: Real power loss minimization

Power loss in transmission systems is inevitable due to the intrinsic resistance of the wires. Therefore, the active power loss is worth considering. The mathematical model of this case is given as follows:

$$F_{Loss} = \sum_{i=1}^{nl} \sum_{i \neq j}^{nl} G_{ij} \cdot [V_i^2 + V_j^2 - 2V_i \cdot V_j \cdot cos(\delta_i - \delta_j)] \tag{16}$$

Case 6: emission and generation cost minimization

The emission cost and generation cost are both considered in this case. The emission and generation costs are formulated as follows:

$$F_{VD} = \sum_{i=1}^{NL} (V_{L_P} - 1.0) \tag{17}$$

Case 7: Fuel cost and real power loss minimization

This multi-objective case is converted to a single objective by multiplying a weight factor by one of the objectives. The problem can be formulated as follows:

$$F_1(X) = \sum_{i=1}^{NG} (a_i \cdot P_{G_i}^2 + b_i \cdot P_{G_i}^2 + c_i) + \lambda_P \cdot F_{Loss} \tag{18}$$

where F_{Loss} is calculated according to Case 5 and the factor of λ_P is set as 40.

Case 8: Fuel cost and voltage deviation minimization

Voltage deviation is a measure of voltage quality in the network. The index of deviation is also vital from a security aspect. The indicator is formulated as the cumulative deviation of the voltages of all load buses (PQ buses) in the network from the nominal value of unity. The formula is as follows

$$F_1(X) = \sum_{i=1}^{NG} (a_i \cdot P_{G_i}^2 + b_i \cdot P_{G_i}^2 + c_i) + \lambda_V D \cdot VD \tag{19}$$

where $\lambda_V D$ is a weighted factor set as 100.

Case 9: Fuel cost and enhancement of voltage stability minimization

The objective function is to minimize the weighted sum of the fuel cost and enhance the voltage stability of the system. The multiple objectives are converted to a single objective, as follows.

$$F_1(X) = \sum_{i=1}^{NG} (a_i \cdot P_{G_i}^2 + b_i \cdot P_{G_i}^2 + c_i) + \lambda_L \cdot L_{max} \tag{20}$$

where Λ_L is the weighted factor set as 100.

Case 10: Fuel cost, emission, voltage deviation and power losses minimization

Four objectives, which are fuel cost, emission, voltage deviation and power losses, are considered in this case.

$$F_1(X) = \sum_{i=1}^{NG} (a_i \cdot P_{G_i}^2 + b_i \cdot P_{G_i}^2 + c_i) + \lambda_E \cdot F_E + \lambda_V D \cdot F_{VD} + \lambda_P \cdot F_{Loss} \tag{21}$$

where three weighted factors are set as $\lambda_E = 19$, $\lambda_V D = 21$ and $\lambda_P = 22$, which can be referred to [21].

3.1.3. Constraints

There are various types of constraints in OPF problems. The active power should be equal to the reactive power, which are equality constraints.

$$\begin{aligned} P_{G_i} - P_{D_i} - V_i \cdot \sum_{j=1}^{NB} V_j \cdot [G_{ij} cos(\delta_i - \delta_j) + B_{ij} sin(\delta_i - \delta_j)] = 0, i = 1, ..., NB \\ Q_{G_i} - Q_{D_i} - V_i \cdot \sum_{j=1}^{NB} V_j \cdot [G_{ij} cos(\delta_i - \delta_j) - B_{ij} sin(\delta_i - \delta_j)] = 0, i = 1, ..., NB \end{aligned} \tag{22}$$

where P_{D_i} represents the active load. Q_{D_i} is the reactive load and δ_i is the i-th bus voltage angle. NB is the number of the buses. G_{ij} and B_{ij} are the transfer conductance and the susceptance between buses i and j, respectively. There are four inequality constraints, which can be presented as follows:

(1) Generator constraints:

$$\begin{aligned} P_{G_i}^{min} \leq P_{G_i} \leq P_{G_i}^{max}, i = 1, .., NG \\ Q_{G_i}^{min} \leq Q_{G_i} \leq Q_{G_i}^{max}, i = 1, .., NG \\ V_{G_i}^{min} \leq V_{G_i} \leq V_{G_i}^{max}, i = 1, .., NG \end{aligned} \tag{23}$$

where the i-th bus generator active power P_{G_i}, reactive power output Q_{G_i} and voltage magnitude at the i-th generator bus V_{G_i} are generated within their lower and upper bounds.

(2) Shunt compensator constraints:

$$Q_{C_j}^{min} \leq Q_{C_j} \leq Q_{C_j}^{max}, j = 1, .., NC \tag{24}$$

where the shunt compensator at the j-th bus Q_{C_j} should lie in its lower and upper limits.

(3) Transformer constraints:

$$T_k^{min} \leq T_k \leq T_k^{max}, k = 1, .., NT \tag{25}$$

where the k-th branch transformer tap T_k is within its lower and upper limits.

(4) Security constraints:

$$\begin{aligned} V_{L_m}^{min} \leq V_{L_m} \leq V_{L_m}^{max}, k = 1, .., NL \\ S_{L_n} \leq S_{L_n}^{max}, n = 1, ..., nl \end{aligned} \tag{26}$$

where the voltage magnitude at the m-th load bus V_{L_m} and n-th line loading should follow its lower and upper bounds.

Experimental Results

The IEEE 30-bus test system is used to test the effectiveness of the algorithm. The system has 6 bus generators, and 24 load buses. The lower bounds of the voltage magnitude is 0.95 p.u. The upper bounds of the PV buses and PQ buses are 1.1 p.u. and 1.05 p.u., respectively. The lower and upper bound of transformer tappings are 0.9 and 1.1 p.u., respectively. The proposed IϵJADE algorithm is compared with state-of-the-art DEs, which are ECHT-DE [22], SF-DE [22], SP-DE [22] and ACDE [1].

3.2. Results of the OPF Problems

In this subsection, the proposed algorithm is compared with ECHT-DE. SF-DE, SP-DE and ACDE. The experimental results are shown in Table 2. It is worth mentioning that the control parameters of the proposed algorithm are the same as ACDE. The biggest difference between ACDE and Iϵ-JADE is the constraint handling technique. ACDE uses the SF method rather than the ϵ constraint method in Iϵ-JADE.The maximum, minimum and average values of thirty independent runs are shown in Table 2. The best results among all the algorithms are marked in boldface.

- For case 1, the simulation results show that ACDE has a better Min values, Max values and Std values than the improved ϵJADE. Improved ϵ-JADE presents better mean values in this case, which indicates that the effectiveness of the proposed algorithm.
- For case 2, case 3, case 5, case 6 and case 10, the proposed improved ϵ-JADE algorithm exhibits a competitive performance on the Min, Max and Mean values when compared with the other four state-of-the-art DE algorithms;
- For case 4, all compared DE algorithms provide the same competitive results.
- For case 8, ACDE and SP-DE achieve the best Mean value, while the improved ϵJADE demonstrates a remarkable performance in terms of the Min value;

- With regard to case 7 and case 9, the proposed improved ϵJADE demonstrates better results in terms of the Mean and Min values.

In addition, the comparison results between the ACDE and improved ϵJADE are shown in the box plot in Figure 1. In the first four cases, the improved ϵJADE and ACDE are equally good. Meanwhile, in case 5 and case 6, the improved ϵJADE demonstrates a better performance.

Table 2. Experimental results of the IϵJADE and the state-of-the-art algorithms.

Case	Algorithm	Min	Max	Mean	Std
Case1	ECHT-DE	800.4148	800.4258	800.4206	0.0026
	SF-DE	800.4131	800.4192	800.4151	0.0015
	SP-DE	800.4293	800.4684	800.4413	0.0100
	ACDE	**800.4113**	**800.4176**	**800.4133**	**0.0015**
	Iϵ-JADE	800.4115	800.4229	800.4135	0.0021
Case2	ECHT-DE	832.1356	832.2239	832.1811	0.0222
	SF-DE	832.0882	832.1291	832.1056	**0.0105**
	SP-DE	832.4813	832.8760	832.6550	0.0963
	ACDE	832.0722	832.3941	**832.0957**	0.0581
	IϵJADE	**832.0698**	**832.1225**	**832.0809**	**0.0109**
Case3	ECHT-DE	0.1363	0.1372	0.1369	0.0002
	SF-DE	0.1367	0.1370	0.1369	0.0001
	SP-DE	0.1374	0.1386	0.1378	0.0002
	ACDE	0.1364	0.1368	0.1366	0.0001
	IϵJADE	**0.1364**	**0.1367**	**0.1365**	**0.0001**
Case4	ECHT-DE	0.2048	0.2048	0.2048	0.0000
	SF-DE	0.2048	0.2048	0.2048	0.0000
	SP-DE	0.2048	0.2048	0.2048	0.0000
	ACDE	0.2048	0.2048	0.2048	0.0000
	IϵJADE	0.2048	0.2048	0.2048	0.0000
Case5	ECHT-DE	3.0850	3.0871	3.0858	0.0005
	SF-DE	3.0845	3.0857	3.0849	0.0003
	SP-DE	3.0844	3.0854	3.0848	0.0003
	ACDE	3.0840	3.0862	3.0845	0.0005
	IϵJADE	**3.0840**	**3.0851**	**3.0844**	0.0003
Case6	ECHT-DE	0.0878	0.0916	0.0893	0.0009
	SF-DE	0.0867	0.0890	0.0880	0.0007
	SP-DE	0.0867	0.0892	0.0877	0.0007
	ACDE	**0.0856**	0.0878	0.0865	0.0007
	IϵJADE	**0.0856**	**0.0884**	**0.0863**	0.0007
Case7	ECHT-DE	1040.1510	1040.2330	1040.1810	0.0213
	SF-DE	1040.1250	**1040.1620**	1040.1400	0.0096
	SP-DE	1040.1340	1040.3370	1040.2390	0.0444
	ACDE	1040.1133	1040.1891	1040.1268	0.0177
	IϵJADE	**1040.1127**	1040.1642	**1040.1245**	0.0115
Case8	ECHT-DE	813.1742	813.4095	814.2470	0.0490
	SF-DE	813.1956	813.3376	813.2585	0.0444
	SP-DE	813.1959	813.2643	**813.2306**	0.0181
	ACDE	813.1100	813.5334	**813.1379**	0.0805
	IϵJADE	**813.1099**	813.5583	813.1462	0.0846
Case9	ECHT-DE	814.1708	814.2001	814.1843	0.0075
	SF-DE	814.1649	**814.1956**	814.1767	0.0063
	SP-DE	814.1841	814.2273	814.2017	0.0121
	ACDE	814.1588	814.2957	814.1897	0.0305
	IϵJADE	**814.1588**	814.2162	**814.1746**	0.0118
Case10	ECHT-DE	964.1331	964.1564	964.1437	0.0061
	SF-DE	964.1254	964.1418	964.1307	0.0038
	SP-DE	964.1234	964.1399	964.1276	0.0034
	ACDE	964.1179	964.1493	964.1252	0.0083
	IϵJADE	**964.1176**	**964.1380**	**964.1227**	0.0050

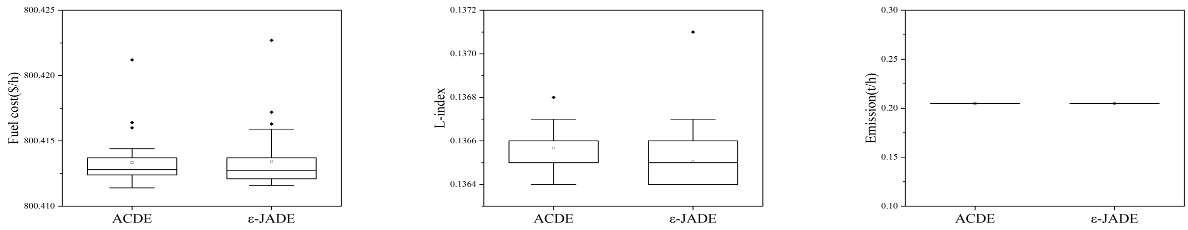

(**a**) Boxplot of case 1 (**b**) Boxplot of case 2 (**c**) Boxplot of case 3

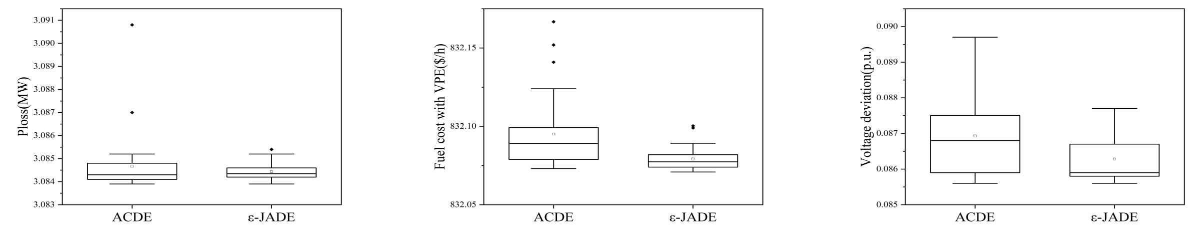

(**d**) Boxplot of case 4 (**e**) Boxplot of case 5 (**f**) Boxplot of case 10

Figure 1. Comparison of IϵJADE and ACDE.

The convergence curves of ACDE and the improved ϵ JADE (ϵ JADE is used for short in the legend) are shown in Figure 2. The figure shows that the improved ϵ JADE has a competitive convergence rate with ACDE. As mentioned above, using the ϵ method will lead to a slow convergence speed towards the feasible region compared with SF. For constrained optimization problems with a relatively small feasible region, the ϵ method is more effective in guiding the population to move toward the feasible region. By considering both target values and constraints, the proposed method will not lead to a significant decrease in the convergence speed.

Based on the comparison results of five DE variants, it is found that the performance of the algorithm, especially the robustness, is significantly improved by the ϵ method.

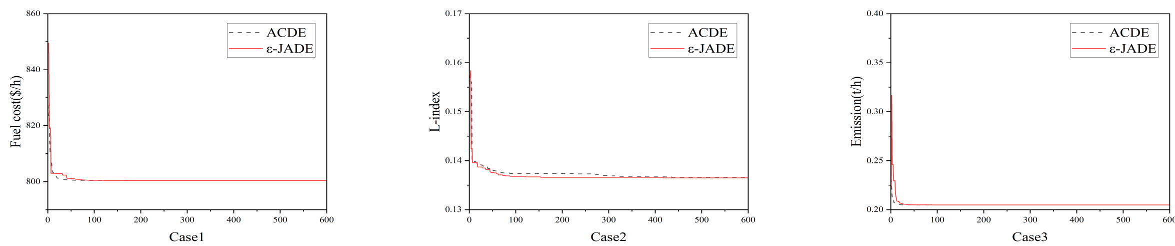

(**a**) Convergence curve of case 1 (**b**) Convergence curve of case 2 (**c**) Convergence curve of case 3

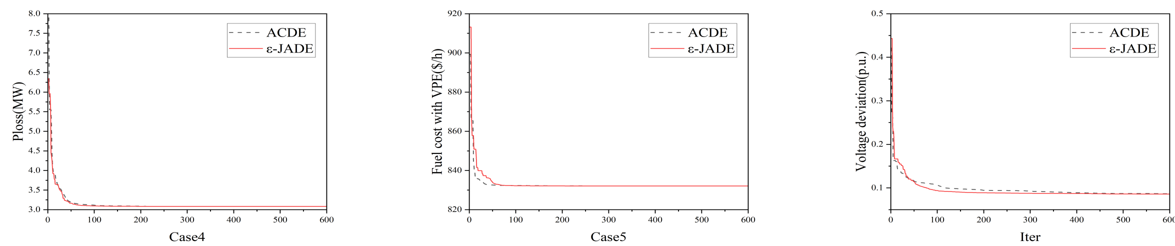

(**d**) Convergence curve of case 4 (**e**) Convergence curve of case 5 (**f**) Convergence curve of case 6

Figure 2. Convergence curve of improved ϵJADE and ACDE.

From the Figure 3, the load bus voltages of different load buses in all the six cases are within bound, which means that the solutions are all feasible. We can observe that the load bus voltage of different load buses follows the same trend, which can help solve other problems in this series.

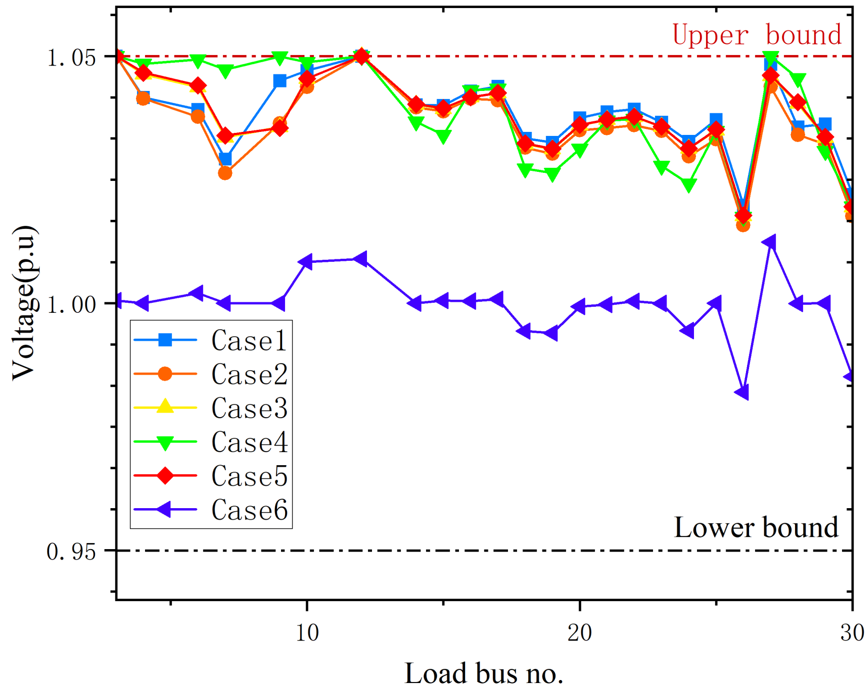

Figure 3. Security graph.

Comparison between Improved ϵJADE and ACDE

The convergence curves of the improved ϵJADE and ACDE in the first six cases are given in Figure 2.

Compared with the ACDE, it can be observed that the proposed improved ϵJADE has a competitive performance with ACDE. The convergence speed of the proposed algorithm is faster than that of ACDE in most cases.

From the boxplots in Figure 1, it can be observed that the proposed algorithm obtains more stable and robust results than ACDE, which illustrates the effectiveness of the improved algorithm.

4. Discussion

Compared with state-of-the-art algorithms in dealing with OPF problems, it can be concluded that the improved ϵ method with the adaptive differential evolution can achieve competitive results. In dealing with the constrained optimization problems, the algorithm is important in searching for the optimal and constraint handling method. The adaptive differential evolution can be applied in solving the constrained optimization problems without extra computations. It is still more efficient in finding the feasible solutions than the classical differential evolution. The proposed selection based on the constraint violation is simple yet effective in improving the algorithm. The ϵ method has shown a great performance in complex constrained optimization problems [23]; meanwhile, it is effective without losing the efficiency through the experimental results in OPF problems. Compared with the simple feasible rules methods, the improved ϵ method can be more suitable in dealing with the complex OPF problems.

5. Conclusions

In this paper, an improved ϵ method based on the adaptive differential evolution is utilized to solve the optimal flow problems. The improved ϵ method can help the algorithm move toward the feasible region, and the improved algorithm is efficient in searching for the feasible global optimum. The effectiveness of the proposed algorithm is tested on the IEEE-30 buses series benchmark functions. Compared with the state-of-the-art algorithms, the performance of the proposed algorithm is competitive in terms of the convergence speed and precision.

In the future, the proposed algorithms could be used to solve more complex optimal flow problems. More effective constraint handling techniques could be combined with the improved adaptive differential evolution algorithms in dealing with the complex constrained optimization problems. It is also promising to implement the machine-learning-based parameter-setting methods within the algorithm rather than fine tuning the control parameters by experiments.

Author Contributions: Conceptualization, W.Y. and Z.L.; methodology and software, W.Y.; validation, Z.L.; investigation, Y.L. and W.Y.; writing—original draft preparation, W.Y. and Z.L.; writing—review and editing, Z.Y.; supervision, S.X.; project administration, Y.C.; funding acquisition, W.Y. All authors have read and agreed to the published version of the manuscript.

Funding: This research was funded by the National Natural Science Foundation of China under Grant Nos. 52005447, 72271222 and Zhejiang Provincial Natural Science Foundation of China under Grant Nos. LQ21E050014, LGG22G010002.

Data Availability Statement: The data presented in this study are available on request from the corresponding author.

Conflicts of Interest: The authors declare no conflict of interest.

References

1. Li, S.; Gong, W.; Hu, C.; Yan, X.; Wang, L.; Gu, Q. Adaptive constraint differential evolution for optimal power flow. *Energy* **2021**, *235*, 121362. [CrossRef]
2. Ida Evangeline, S.; Rathika, P. Wind farm incorporated optimal power flow solutions through multi-objective horse herd optimization with a novel constraint handling technique. *Expert Syst. Appl.* **2022**, *194*, 116544. [CrossRef]
3. Bouchekara, H. Solution of the optimal power flow problem considering security constraints using an improved chaotic electromagnetic field optimization algorithm. *Neural Comput. Appl.* **2020**, *32*, 2683–2703. [CrossRef]
4. Mugemanyi, S.; Qu, Z.; Rugema, F.X.; Dong, Y.; Bananeza, C.; Wang, L. Optimal Reactive Power Dispatch Using Chaotic Bat Algorithm. *IEEE Access* **2020**, *8*, 65830–65867. [CrossRef]
5. Saha, A.; Bhattacharya, A.; Das, P.; Chakraborty, A.K. HSOS: A novel hybrid algorithm for solving the transient-stability-constrained OPF problem. *Soft Comput.* **2020**, *24*, 7481–7510. [CrossRef]
6. Farhat, M.; Kamel, S.; Atallah, A.M.; Hassan, M.H.; Agwa, A.M. ESMA-OPF: Enhanced Slime Mould Algorithm for Solving Optimal Power Flow Problem. *Sustainability* **2022**, *14*, 2305. [CrossRef]
7. Abd el sattar, S.; Kamel, S.; Ebeed, M.; Jurado, F. An improved version of salp swarm algorithm for solving optimal power flow problem. *Soft Comput.* **2021**, *25*, 4027–4052. [CrossRef]
8. Akdag, O. A Improved Archimedes Optimization Algorithm for multi/single-objective Optimal Power Flow. *Electr. Power Syst. Res.* **2022**, *206*, 107796. [CrossRef]
9. Abbasi, M.; Abbasi, E.; Mohammadi-Ivatloo, B. Single and multi-objective optimal power flow using a new differential-based harmony search algorithm. *J. Ambient Intell. Humaniz. Comput.* **2021**, *12*, 851–871. [CrossRef]
10. Teeparthi, K.; Vinod Kumar, D.M. Security-constrained optimal power flow with wind and thermal power generators using fuzzy adaptive artificial physics optimization algorithm. *Neural Comput. Appl.* **2018**, *29*, 855–871. [CrossRef]
11. El-Fergany, A.A.; Hasanien, H.M. Salp swarm optimizer to solve optimal power flow comprising voltage stability analysis. *Neural Comput. Appl.* **2020**, *32*, 5267–5283. [CrossRef]
12. Naderi, E.; Pourakbari-Kasmaei, M.; Cerna, F.V.; Lehtonen, M. A novel hybrid self-adaptive heuristic algorithm to handle single- and multi-objective optimal power flow problems. *Int. J. Electr. Power Energy Syst.* **2021**, *125*, 106492. [CrossRef]
13. Elattar, E.E.; Shaheen, A.M.; Elsayed, A.M.; El-Sehiemy, R.A. Optimal Power Flow With Emerged Technologies of Voltage Source Converter Stations in Meshed Power Systems. *IEEE Access* **2020**, *8*, 166963–166979. [CrossRef]
14. Kahraman, H.T.; Akbel, M.; Duman, S. Optimization of Optimal Power Flow Problem Using Multi-Objective Manta Ray Foraging Optimizer. *Appl. Soft Comput.* **2022**, *116*, 108334. [CrossRef]

15. Attia, A.F.; El Sehiemy, R.A.; Hasanien, H.M. Optimal power flow solution in power systems using a novel Sine-Cosine algorithm. *Int. J. Electr. Power Energy Syst.* **2018**, *99*, 331–343. [CrossRef]
16. Nguyen, T.T.; Mohammadi, F. Optimal Placement of TCSC for Congestion Management and Power Loss Reduction Using Multi-Objective Genetic Algorithm. *Sustainability* **2020**, *12*, 2813. [CrossRef]
17. Mohamed, A.A.; Kamel, S.; Hassan, M.H.; Mosaad, M.I.; Aljohani, M. Optimal Power Flow Analysis Based on Hybrid Gradient-Based Optimizer with Moth–Flame Optimization Algorithm Considering Optimal Placement and Sizing of FACTS/Wind Power. *Mathematics* **2022**, *10*, 361. [CrossRef]
18. Gong, W.; Cai, Z. Differential evolution with ranking-based mutation operators. *IEEE Trans. Cybern.* **2013**, *43*, 2066–2081. [CrossRef]
19. Takahama, T.; Sakai, S. Constrained optimization by the ε constrained differential evolution with gradient-based mutation and feasible elites. In Proceedings of the 2006 IEEE International Conference on Evolutionary Computation, Vancouver, BC, Canada, 16–21 July 2006; pp. 1–8.
20. Zitzler, E. *Evolutionary Algorithms for Multiobjective Optimization: Methods and Applications*; Ithaca: Shaker, OH, USA, 1999; Volume 63.
21. Mohamed, A.A.A.; Mohamed, Y.S.; El-Gaafary, A.A.; Hemeida, A.M. Optimal power flow using moth swarm algorithm. *Electr. Power Syst. Res.* **2017**, *142*, 190–206. [CrossRef]
22. Biswas, P.P.; Suganthan, P.N.; Mallipeddi, R.; Amaratunga, G.A. Optimal power flow solutions using differential evolution algorithm integrated with effective constraint handling techniques. *Eng. Appl. Artif. Intell.* **2018**, *68*, 81–100. [CrossRef]
23. Yi, W.; Gao, L.; Pei, Z.; Lu, J.; Chen, Y. ε Constrained differential evolution using halfspace partition for optimization problems. *J. Intell. Manuf.* **2021**, *32*, 157–178. [CrossRef]